Chiral Discrimination in the ^{13}C and ^{2}H NMR of the Crown and Saddle Isomers of Nonamethoxy-Cyclotriveratrylene in Chiral Liquid-Crystalline Solutions

Olivier Lafon,[†,||] Philippe Lesot,*[,†] Herbert Zimmermann,[‡] Raphy Poupko,[§] and Zeev Luz*[,§]

Laboratoire de Chimie Structurale Organique, Equipe RMN en Milieu Orienté, ICMMO, CNRS UMR 8182, Bât. 410, Université de Paris-Sud (XI), 91405 Orsay, France, Abteilung Biophysik, Max-Planck-Institut für Medizinische Forschung, Jahnstrasse 29, 69120 Heidelberg, Germany, and Department of Chemical Physics, Weizmann Institute of Science, Rehovot 76100, Israel

Received: January 23, 2007; In Final Form: April 10, 2007

We report ^{2}H and ^{13}C NMR spectra of the crown and saddle isomers of nonamethoxy-tribenzocyclononene (**1**), dissolved in lyotropic achiral and chiral liquid-crystalline solutions based on poly-γ-benzyl-glutamate and poly-γ-benzyl-L-glutamate (PBG and PBLG). The $^{2}H-\{^{1}H\}$ measurements include spectra of compound **1** deuterated in the ring methylene and in the aromatic sites as well as of the methyl groups in natural abundance. Carbon-13 spectra were recorded in natural abundance as well as in two isotopomers enriched in the ring methylene and one of the methoxy groups. The crown isomer (c-**1**) is rigid with C_3 symmetry and can be separated into its enantiomers using a chiral high-performance liquid chromatography column. The NMR spectra of racemic c-**1** in PBLG solutions exhibit two sets of lines due to the enantiomers. The peaks were identified by comparing the spectra with those of the neat enantiomers. Analysis of the ^{2}H quadrupolar splittings and the ^{13}C residual chemical shift anisotropies shows that the dominant factor determining the chiral discrimination is the difference in the ordering of the two enantiomers in the chiral liquid crystals. The saddle isomer (s-**1**) is highly flexible, undergoing fast pseudorotation between six conformers. The "frozen" conformers have C_1 symmetry and are therefore chiral. Three of these comprise one enantiomer, and the other three the second one. However, the rapidly interconverting species has, on the average, a C_{3h} symmetry and is therefore achiral. The methylene groups in the latter are, however, prostereogenic, and their hydrogen/deuterium−carbon bonds constitute enantiotopic pairs. The ^{2}H NMR spectra of the s-**1** methylene-deuterated in PBLG solutions exhibit, in fact, enantio-discrimination with two quadrupolar doublets. This is in contrast to rigid prochiral molecules with a threefold symmetry axis, which normally do not show such discrimination. A detailed analysis of the effect is presented, and it is argued that the discrimination observed for s-**1** reflects the different ordering of its enantiomers during the pseudorotation cycle.

Introduction

This work is a sequel to our earlier publication[1] on the ordering characteristics of substituted tribenzo-cyclononatriene (TBCN) dissolved in lyotropic chiral liquid crystals made of poly-γ-benzyl-L-glutamate (PBLG). The TBCN derivatives are often named, after their parent compound, hexamethoxy-TBCN, cyclotriveratrylenes (CTVs).[2] When the substitution pattern of the CTV core results in conformations lacking planes of symmetry, the compounds become structurally chiral, and their NMR spectrum in chiral solvents may show enantioseparation. This was apparently first detected in the ^{1}H spectrum of the racemic crown form of nonamethoxy-TBCN in dimethylsulfoxide solutions containing a chiral Eu(III) shift reagent, but no details were provided.[3] In ref 1 we studied the ^{2}H and ^{13}C NMR spectra of this compound in achiral and chiral lyotropic liquid-crystalline solutions based on poly-γ-benzyl-glutamate. While in achiral solvents a single set of lines was observed for the various nuclei, two sets were observed for most nuclei in the chiral solvent. The two sets correspond, respectively, to the M and P enantiomers of the crown form as defined in Figure 1a.

Since the publication of this work, two important new observations regarding nonamethoxy-TBCN were made.[4] The first concerns its enantioseparation. It was found that, using a suitable chiral high-performance liquid chromatography (HPLC) column, it is possible to quantitatively separate the racemate into its enantiomers. In the present work we extend the study of the ordering characteristics of nonamethoxy-TBCN in liquid-crystalline solutions to the neat enantiomers. To that end we have synthesized several isotopomers of the crown form, separated them into their enantiomers, and studied their ^{13}C and ^{2}H NMR spectra in both chiral[5] and achiral[6] liquid-crystalline solutions. As in ref 1, the former and latter consisted, respectively, of poly-γ-benzyl-L-glutamate (PBLG) and equal mass mixtures of PBLG and poly-γ-benzyl-D-glutamate (PBDG) (henceforth referred to as PBG) dissolved in suitable organic cosolvents. The degrees of polymerization (DPs) of the two polypeptides were similar (782 and 914, respectively), and the cosolvents used in the present work were dimethylformamide (DMF) and tetrahydrofuran (THF). The PBLG solutions form,

* Author to whom the correspondence should be addressed. Phone: +33 (0)1 69 15 47 59 (P.L.); +972(0)8 934 2020 (Z.L.). Fax: +33 (0)1 69 15 81 05 (P.L.); +972(0)8 934 4123 (Z.L.). E-mail: philesot@icmo.u-psud.fr; zeev.luz@weizmann.ac.il.

† Université de Paris-Sud (XI).

‡ Max-Planck-Institut für Medizinische Forschung.

§ Weizmann Institute of Science.

|| Current address: Laboratoire de Structure et Dynamique par Résonance Magnétique, DSM/DRECAM/SCM, CEA/CNRS URA 331, CEA Saclay, 91191 Gif-sur-Yvette Cedex, France.

10.1021/jp070564q CCC: $37.00
Published on Web 07/21/2007

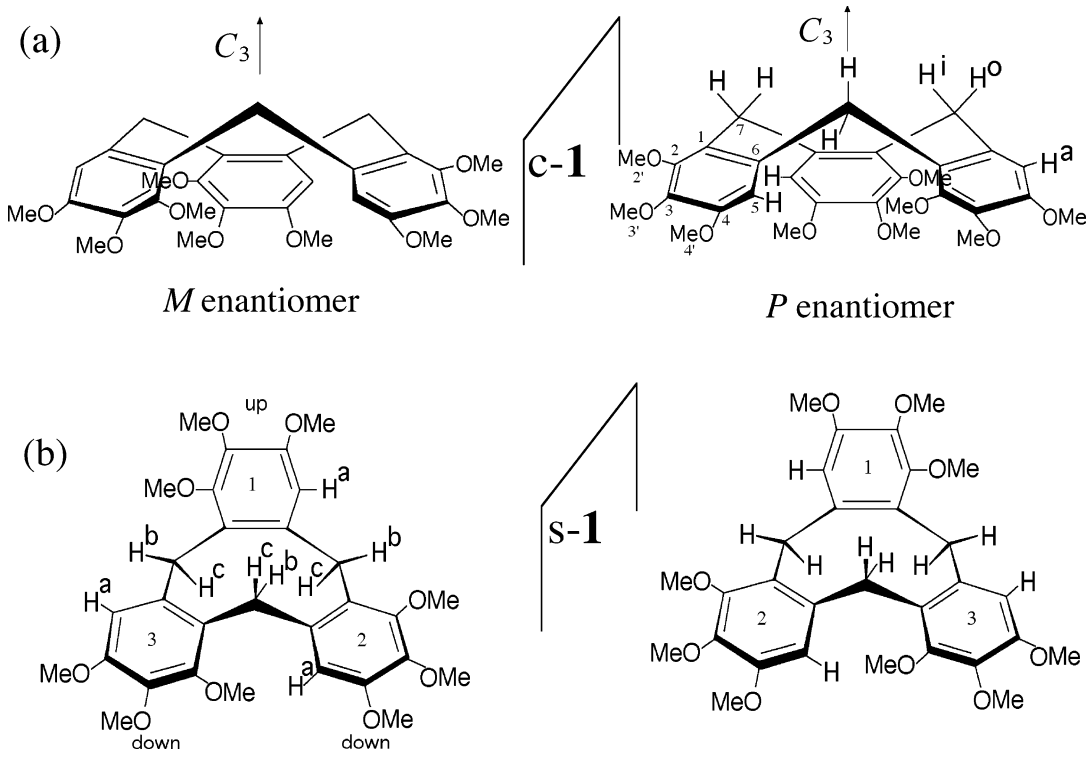

Figure 1. Structures and numbering of the enantiomers of (a) the crown form of **1**, c-**1**, and (b) the "frozen" saddle form, s-**1**. The left diagram of part b corresponds to the reference conformer I in Figure 10, with a, b, and c labeling the aromatic and methylene deuterons (see text). The structure on the right-hand side of part b corresponds to conformer IV of Figure 10 (rotated by 180° about a vertical axis in the paper plane).

in fact, cholesteric liquid crystals (CLCs), but their pitch is unwound in the magnetic field of the NMR spectrometer, resulting in a chiral nematic phase with the director aligned parallel to the magnetic field. However, the racemic PBG solutions form achiral nematic phases, which, likewise, align with their director parallel to the magnetic field. The results, so obtained with neat enantiomers, allow us to associate the different NMR peaks with one or the other enantiomers and to compare their different degrees of ordering in the CLC solutions. It is hoped that such data may eventually be used to relate the ordering properties of the enantiomers to their absolute configurations.

The other new observation on nonamethoxy-TBCN concerns its saddle form. Contrary to earlier reports,[7] it was found[4] that this isomer (Figure 1b) can in fact be prepared and separated from the crown isomer. As it happens, the separation can be effected using the same HPLC column as used for the enantiomeric separation of the crown antipodes. The situation is thus similar to that for the (achiral) parent CTV compound, which, also contrary to earlier thoughts, does exhibit a stable saddle form.[8] At room temperature the crown−saddle equilibration in solution is very slow ($t_{1/2} \approx$ several months) and essentially infinite in the solid state, thus allowing the separate study of the two isomers. Unlike the rigid crown form, the saddle isomer is highly flexible, undergoing extremely fast pseudorotation in solution. In the hexamethoxy analogue this process could not be frozen out on the NMR time scale, even by cooling down to very low temperatures.[8] The "frozen" conformers of the saddle isomer of nonamethoxy-TBCN are, of course, also chiral, but the fast pseudorotation process results in complete racemization. Consequently, the NMR spectrum of the saddle isomer corresponds to that of a single species with an "average" C_{3h} symmetry (achiral). In using the notion of an "average structure" or "average symmetry" for a flexible molecule, we use Altmann's definition.[9] According to this definition the average symmetry of a flexible molecule is the semidirect product of the "isodynamic group", the group consisting of the set of dynamic processes, and the symmetry group of the "frozen" molecule. For the saddle isomer of nonamethoxy-TCBN the group of interconversion processes is isomorphic with the C_{3h} group (see below), while the symmetry of a single conformer is C_1. Hence, the average symmetry of the saddle isomer is $C_{3h} \otimes C_1 = C_{3h}$. The ring methylene hydrogens in this average structure are enantiotopically related, and their deuterium NMR spectra in CLC solutions in fact exhibit enantiotopic discrimination. Such discrimination is usually not observed in rigid prochiral molecules possessing a C_3 symmetry axis. This is so because in such molecules the C_3 axis is retained when dissolved in CLC, and in the absence of strong distorting forces (which would distort the molecular geometry), the enantiotopic sites remain equivalent. It will be shown that the origin of the chiral discrimination in the flexible saddle isomer results from the orientational properties of the individual (chiral) conformers during the pseudorotation cycle.

Hereafter we label the compound nonamethoxy-TBCN as **1** and its crown and saddle isomers as c-**1** and s-**1**, respectively. The enantiomers of the crown isomer will be labeled as A and B according to the order of their elution from the HPLC columns (A, first, and B, second). Meanwhile we have, in fact, found, using vibration circular dichroism spectroscopy,[3,4] that these two enantiomers correspond, respectively, to configurations P and M of Figure 1a. In the present paper we shall, however, continue to refer to them as A and B.

Materials and Methods

Synthesis and Isomeric Separation of the Isotopically Normal 1. Isotopically normal c-**1** was synthesized by acid condensation (10% sulfuric acid) of 3,4,5-trimethoxy benzyl alcohol as described earlier.[1] After chromatographic purification the resulting material consisted of the pure racemic crown form.

It was separated into its enantiomers by HPLC, using a semipreparative column (25 cm × 2 cm i.d.) packed with 5 μm silica particles coated with a polysaccharide as the chiral stationary phase (CHIRALCEL OD-H, Chiral Technologies Europe). A 1:1 acetonitrile/methanol mixture served as the injection solvent, and a 1:1 ethanol/methanol mixture as the mobile phase. Two well-separated peaks were obtained in the chromatogram due to the enantiomers of c-**1**. We labeled them A and B, according to the order of their elution from the separation columns.

To obtain s-**1** a solution of c-**1** in the high-boiling-point solvent, tetraethylene glycol dimethyl ether (tetraglyme) was heated to 265 °C for several minutes. At this temperature the crown−saddle equilibrium ratio is approximately 1:1. The hot solution was splashed into an ice/salt mixture and then allowed to warm up to room temperature. The crown−saddle mixture was filtered, dissolved in methylene chloride, and dried by pumping at room temperature. The neat saddle isomer was finally separated from the mixture by HPLC, using the same columns and procedure as used for separating the enantiomers of the crown form.

Preparation of the Isotopomers of 1. Several isotopomers of **1** were synthesized in the crown form and then used to prepare the corresponding isotopically labeled enantiomers as well as the corresponding saddle isotopomers as described above. Two deuterated isotopomers of **1** were prepared: (i) **1** deuterated in the ring methylene (**1**-CD_2) and (ii) **1** deuterated in the unsubstituted aromatic site (**1**-CD). The first of these was prepared by condensation of the corresponding deuterated trimethoxy benzyl alcohol, which was prepared by reduction of 3,4,5-trimethoxy benzoic acid with $LiAlD_4$ in THF under reflux. The second isotopomer, **1**-CD, was prepared from the normal compound by exchange with CF_3COOD at room temperature (20 h). The solution was evaporated near ambient temperature, thus yielding a dark yellow oil that was dried on a vacuum manifold at 10 Torr. The oil was triturated with a few drops of D_2O and ether and stirred for 2 h. The solution turned colorless, yielding white crystals of the desired compound. In the actual experiments described below solutions containing equal amounts of **1**-CD_2 and **1**-CD were used.

In addition two ^{13}C isotopomers were prepared: (i) **1** labeled in the ring methylene (**1**-$^{13}CH_2$) and (ii) **1** enriched to 50% in ^{13}C in the central methoxy group, 3′ (**1**-$O^{13}CH_3$). Both were prepared from their respective ^{13}C-labeled benzyl alcohol. The precursor for **1**-$^{13}CH_2$ was prepared by first cyanating 3,4.5-trimethoxy bromobenzene with $Cu^{13}CN$ (made from $CuCl_2$ and $K^{13}CN$ in water) in DMF at 160 °C. The resulting benzonitrile was hydrolyzed under reflux in a NaOH solution to yield the sodium salt of the corresponding ^{13}C-labeled benzoic acid. After separating the free acid it was reduced to the corresponding alcohol by $LiAlH_4$ in THF. The precursor for **1**-$O^{13}CH_3$ was prepared by alkylation of 3,5-dimethoxy-4-hydroxy benzyl alcohol with CH_3I (50% ^{13}C) in a boiling acetone solution of K_2CO_3.

Preparation of the Liquid-Crystalline Samples. The liquid-crystalline media consisted of solutions of PBG or PBLG in either DMF or THF. The NMR measurements were made on solutions containing weighed amounts of the various isotopomers of **1** in the above solvents. A typical composition of such solutions consists of 27−30 wt % poly-γ-benzyl-glutamate and about 1 wt % solute in the organic cosolvent. The solutions were placed in 5 mm NMR tubes, fire-sealed, and centrifuged several times, with the directions of the tubes alternately up and down, until a homogeneous phase was obtained. The exact composition of the various samples is given in Table 1. Other details can be found in refs 5, 6, 8, and 10.

NMR Measurements. The carbon-13 magic-angle spinning (MAS) NMR spectra of the solid c-**1** sample were recorded on a DSX-300 Bruker spectrometer equipped with a 5 mm MAS probe and operating at 75.4 MHz. The $^2H-\{^1H\}$ and $^{13}C-\{^1H\}$ NMR spectra in liquid crystal phases were performed on a 9.4 T Bruker Avance spectrometer (400.1 MHz) equipped with a 5 mm broad-band or quadruple resonance (^1H, ^2H, ^{13}C, ^{15}N) probe. The natural abundance deuterium (NAD) NMR spectra of the isotopically normal compounds were performed on a 600 MHz Bruker Avance spectrometer equipped with a 5 mm ^1H, ^2H dual cryoprobe. The sample temperature was controlled by the Bruker variable temperature controller. For each temperature, the tuning and the matching of the deuterium coil were optimized. The WALTZ-16 sequence was used to decouple protons (<0.5 W of power). Other details are given in the figure captions. The estimated accuracies of the δ and J values in isotropic solvent are ±0.01 ppm and ±0.5 Hz.

Results and Discussion

NMR Spectra of 1 in Isotropic Solvents. To facilitate the interpretation of the NMR spectra of c-**1** and s-**1** in the liquid-crystalline PBG and PBLG solutions, we first analyzed their ^1H and ^{13}C spectra in regular (isotropic) organic solvents. Examples of spectra in DMF-d_7 with their peak assignments are shown in Figure 2. The derived chemical shifts and various J-couplings are summarized in Table 2. Similar values were obtained in $CDCl_3$ and THF-d_8. The assignment was aided by various spectroscopic methods, including $^{13}C-^1H$ correlation experiments (heteronuclear multiple-bond correlation HMBC, and heteronuclear multiple-quantum coherence, HMQC), $^{13}C-^{13}C$ INADEQUATE, and (see below) natural abundance $^2H-\{^1H\}$ Q-resolved experiments with z-gradient filter (Q-resolved Fz) in PBLG solutions.[11,12] Some of the parameters could only be obtained (directly or indirectly) using the ^{13}C-labeled isotopomers, **1**-$^{13}CH_2$ and **1**-$O^{13}CH_3$. For example, the $^{13}C-\{^1H\}$ NMR spectrum of c-**1**-$^{13}CH_2$ allowed us to distinguish the C1 and C6 signals from other quaternary carbon signals, while the INADEQUATE two-dimensional (2D) map allows the unequivocal assignment of the C1 and C6 peaks.[13] In the same way, the ^1H and ^{13}C resonances of the methoxy 3′ groups were assigned by using **1**-$O^{13}CH_3$. The ^1H signals of the methoxy 2′ and 4′ groups could then be identified through $^{13}C-^1H$ HMBC and HMQC 2D experiments.

Deuterium NMR Spectra of the Crown Isomer in Liquid-Crystalline Solutions. In this section we discuss deuterium NMR spectra of racemic mixtures as well as of neat enantiomers (or mixtures thereof) of c-**1** in achiral PBG and chiral PBLG solutions. In trace a of Figure 3 is shown a spectrum of a racemic mixture consisting of a nearly equimolar mixture of c-**1**-CD_2 and c-**1**-CD dissolved in the achiral PBG/DMF solvent. Three doublets are observed, centered at different chemical shifts, δ, and exhibiting different quadrupole splittings, $\Delta\nu_Q^i$, as outlined in the first rows of Table 3a. In this table, as in the rest of the paper, a, i, and o refer, respectively, to the aromatic, inner methylene, and outer methylene hydrogens of c-**1** (Figure 1a). Note that the difference in the peak intensities of the diastereotopic deuterons 7o and 7i originates from a difference in their line widths. The signs of these splitttings, as given in Table 3a, cannot be derived directly from the one-dimensional (1D) spectrum shown in Figure 3a, but they can be deduced by combining the above results with those of the corresponding C−H dipolar splitting observed in proton-coupled ^{13}C spectra in similar liquid-crystalline solutions. The arguments are as fol-

TABLE 1: Labeling and Composition of the Liquid-Crystalline Samples

sample	solute[a]	PBLG[b]/mg[c]	PBDG[b]/mg[c]	solute A/B[d]/mg[c]	DMF/mg[c]	THF/mg[c]	wt % of polymer
1a	c-**1**-CD_2 c-**1**-CD	65	65	2.5/2.5	310	0	29.2
1b	c-**1**-CD_2 c-**1**-CD	60	61	2.8/2.8	0	320	27.1
2a	c-**1**-CD_2 c-**1**-CD	131	0	2.5/2.5	310	0	29.4
2b	c-**1**-CD_2 c-**1**-CD	120	0	2.5/2.5	0	320	27.0
3a	c-**1**-CD_2 c-**1**-CD	129	0	1.3/3.8	312	0	29.2
3b	c-**1**-CD_2 c-**1**-CD	120	0	1.4/4.1	0	321	26.8
4	c-**1**-CD_2 c-**1**-CD	136	0	5/0	312	0	30.0
5	c-**1**-CD_2 c-**1**-CD	136	0	0/5	312	0	29.4
6	c-**1**	210	0	4/4	484	0	29.9
7a	c-**1**	65	65	2.5/2.5	310[e]	0	29.2
7b	c-**1**	60	61	2.5/2.5	0	321[e]	27.1
8a	c-**1**	131	0	2.5/2.5	310[e]	0	29.3
8b	c-**1**	120	0	2.5/2.5	0	320[e]	27.0
9	c-**1**	129	0	1.5/4.5	310[e]	0	29.1
10	c-**1**	130	0	5/0	310[e]	0	29.2
11	c-**1**	129	0	0/5	310[e]	0	29.2
12a	s-**1**	66	65	5	311[e]	0	29.3
12b	s-**1**	61	61	5	0	319[e]	27.3
13a	s-**1**	130	0	5	312[e]	0	29.1
13b	s-**1**	119	0	5	0	320[e]	26.8
14a	s-**1**-CD_2 s-**1**-CD	65	65	5	310	0	29.2
14b	s-**1**-CD_2 s-**1**-CD	60	61	5	0	320	27.1
15a	s-**1**-CD_2 s-**1**-CD	130	0	5	310	0	29.2
15b	s-**1**-CD_2 s-**1**-CD	121	0	6	0	319	27.1

[a] The deuterated solutes consist of approximately equal amounts of the isotopomers labeled in the aromatic site (**1**-CD) and ring methylene site (**1**-CD_2). [b] The DP of PBLG and PBDG is 782 ($M_w \approx 171\,300$) and 914 ($M^w \approx 200\,200$). [c] The accuracy of the weighing is 1 mg. [d] A/B refers to enantiomers A and B of c-**1**. For s-**1**, it is always a racemic mixture. [e] Deuterated cosolvent, DMF-d_7 or THF-d_8, otherwise isotopically normal cosolvents were used.

lows:[1] Assuming axial symmetry of the quadrupolar interaction (and a C_3 molecular symmetry for the crown form) the quadrupole splitting of a deuteron in a C−D bond is given by

$$\Delta\nu_Q^j = \frac{3}{2}Q_{C-D}S_{zz}\left(\frac{3\cos^2(\beta^j)-1}{2}\right) \quad (1)$$

where S_{zz} is the molecular order parameter of the solute, Q_{C-D} is the deuterium quadrupole interaction constant in the particular C−D bond (∼170 and ∼190 kHz for aliphatic and aromatic deuterons, respectively), and β^j is the angle between the C−D bond direction and the molecular C_3 symmetry axis. In Table 3b are given the C5−H splittings, $^1T_{C5-H}$, observed in the (proton-coupled) ^{13}C spectra (inset in Figure 5a) of isotopically normal c-**1** in the same solvents and temperatures as used for recording the ^2H spectra. These splittings correspond to the following combination of the C5−H scalar ($^1J_{C5-H}$) and dipolar ($^1D_{C5-H}$) interactions[5,14−16]

$$^1T_{C5-H} = {}^1J_{C5-H} + 2{}^1D_{C5-H} \quad (2)$$

where the latter is given by

$$^1D_{C-H} = -S_{zz}\left(\frac{K_{C-H}}{r_{C-H}{}^3}\right)\left(\frac{3\cos^2(\beta^{C-H})-1}{2}\right) \quad (3)$$

In this equation, r_{C-H} is the C−H internuclear distance (∼1.09 Å for the C5−H pair), β^{C-H} is the angle between the C−H bond direction and the molecular C_3 axis (essentially the same as β^j in eq 1 and is 90° for the C5−H bond), and K_{C-H} is the dipolar interaction constant for the C−H pair (30.188 Hz Å^3). In principle, it should be possible to calculate $^1D_{C5-H}$ from the measured $^1T_{C5-H}$ value, using eq 2, except that only its magnitude is measured ($|^1T_{C5-H}| = 195$ Hz in PBG/DMF) and not its sign. We note, however, that from eqs 1 and 3 the ratio of the deuterium quadrupolar splitting to that of the C−H dipolar one

$$\frac{\Delta\nu_Q^{C-D}}{^1D_{C-H}} = -\frac{3}{2}Q_{C-D}\left(\frac{r_{C-H}{}^3}{K_{C-H}}\right) \quad (4)$$

is approximately −12.5 for aromatic hydrogens. Thus, from the known value of $|\Delta\nu_Q^{C-D}|$ (2011 Hz, Table 3a), it follows that $|^1D_{C5-H}| \approx 170$ Hz. Since $^1J_{C5-H} = +160$ Hz (Table 2b) (where the + sign is the generally accepted sign for directly bonded C−H pairs), the only consistent solution of eq 2 corresponds to $^1T_{C5-H} = -195$ Hz and $^1D_{C5-H} = -177$ Hz, as given in Table 3b. From eqs 1 and 4 it also follows that the sign of $\Delta\nu_Q^{C5-D}$ is positive and that of S_{zz} is negative (as given in Table 3a). The negative sign of S_{zz} reflects the fact that the solute molecules prefer to align with their C_3 axes perpendicular to the director.

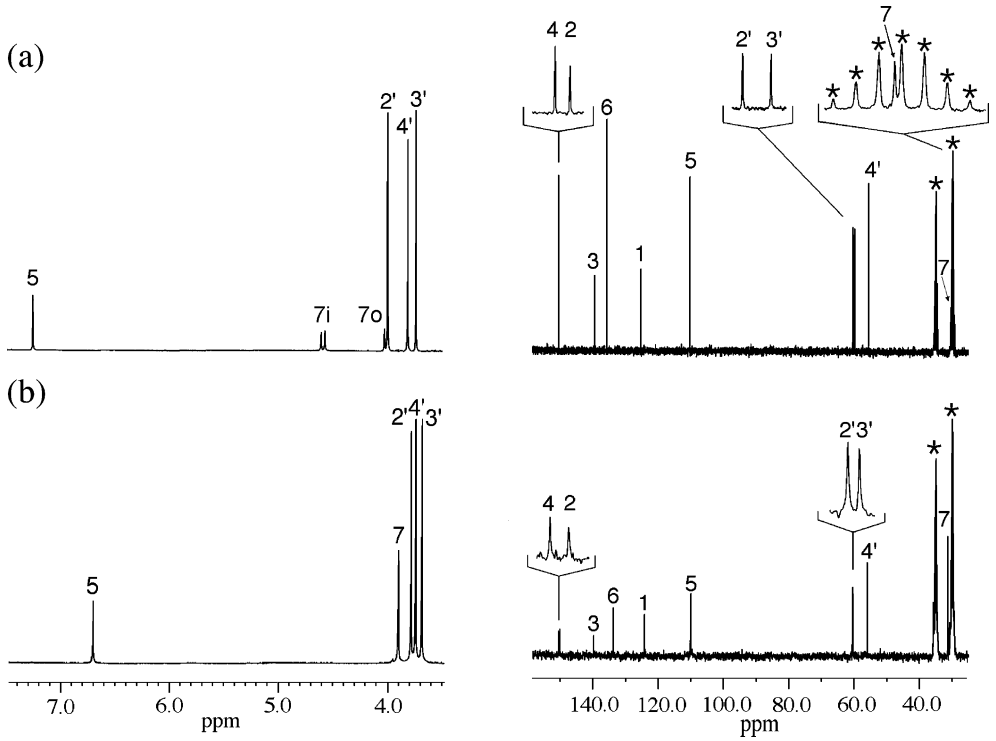

Figure 2. 400.1 MHz ^{1}H (left) and 100.6 MHz ^{13}C−{^{1}H} (right) NMR spectra of the (a) crown and (b) saddle isomers of **1** dissolved in DMF-d_7 at room temperature. Expanded regions are shown for closely spaced peaks in the ^{13}C spectra. Peaks labeled with asterisks correspond to DMF-d_7.

TABLE 2: ^{13}C and ^{1}H Chemical Shifts and *J*-Couplings of the Crown and Saddle Isomers of 1 in DMF-d_7 Solutions

(a) ^{1}H Chemical Shifts[a] (in ppm)

	aromatic site	methylene site		methyl site		
isomer	5	7i	7o	2′	3′	4′
crown (c-**1**)	7.25	4.56[b]	4.00[b]	3.99[c]	3.72[d]	3.80[c]
saddle (s-**1**)	6.70	3.94		3.82[e]	3.72[e]	3.78[e]

(b) ^{13}C Chemical Shifts (in ppm) and $^1J_{C-H}$ Couplings (in Hz)

		aromatic site						methylene site	methyl site		
isomer	spectral parameters	1	2	3	4	5	6	7	2′	3′	4′
crown (c-**1**)	δ[f]	125.37[g]	152.12[h]	141.14[h]	152.2[i]	111.17[j]	136.95[g,i]	30.16[g]	60.94[h]	60.53[k]	56.08[h]
	$^1J_{C-H}$[j]					159.7		127.5[n]	144.2	144.2	144.1
saddle (s-**1**)	δ[f,l]	125.64	152.15	141.59	152.46	111.22	135.53	31.48	60.86	60.70[m]	56.24
	$^1J_{C-H}$[j]					157.4		128.0	144.0	144.0	144.1

(c) Additional Relevant $^nJ_{X-Y}$ couplings (in Hz) for c-**1**

$^2J_{7H(i)-7H(o)}$	$^1J_{C1-C7}$	$^1J_{C6-C7}$	$^1J_{C1-C2}$	$^1J_{C2-C3}$	$^1J_{C3-C4}$	$^1J_{C4-C5}$	$^1J_{C5-C6}$	$^1J_{C6-C1}$	$^2J_{C3'-C3}$	$^3J_{C7-H5}$
13.9	44.5[g]	44.5[g]	69.1	78.2	76.1	67.1	59.5	61.2	1.9[k]	4.7

[a] The most shielded ^{1}H signal of DMF is used as an internal reference at 2.74 ppm. [b] The assignment to 7i and 7o is based on that of the deuterons in CLCs (see text). [c] The assignment is based on ^{13}C−^{1}H correlation 2D experiments (HMQC and HMBC). [d] The assignment is based on the ^{1}H spectrum of c-**1**-O^{13}CH$_3$. [e] The assignment for s-**1** is based on similarity with the crown results. [f] The most shielded ^{13}C signal of DMF-d_7 is used as an internal reference at 30.1 ppm. [g] On the basis of the ^{13}C spectrum of c-**1**-^{13}CH$_2$. [h] On the basis of ^{13}C−^{1}H 2D correlation spectroscopy (HMQC and HMBC). [i] On the basis of the INADEQUATE 2D spectrum. [j] On the basis of the proton-coupled ^{13}C spectrum. [k] On the basis of the ^{13}C spectrum of c-**1**-O^{13}CH$_3$. [l] On the basis of similarity with the crown values. [m] On the basis of the spectrum of enriched s-**1** (s-**1**-O^{13}CH$_3$). [n] Equal values for $^1J_{C7-H(i)}$ and $^1J_{C7-H(o)}$.

In a similar manner we have also analyzed the quadrupole splittings of the ring methylene deuterons (7i and 7o). From the known geometry of the CTV core the angles β^i and β^o can be estimated as 38° and 66°, respectively.[17] Inserting these values in eq 1 immediately identifies the larger and smaller splittings as due to the i and o deuterons, respectively, as indicated in trace a of Figure 3. In fact the ^{1}H chemical shifts of 7i and 7o of Table 2a are based on this assignment. Moreover, recalling that $S_{zz} < 0$, it follows that the signs of $\Delta\nu_Q^i$ and $\Delta\nu_Q^o$ are, respectively, negative and positive as indicated in Table 3a.

We next discuss the deuterium spectrum of deuterated c-**1** (c-**1**-CD + c-**1**-CD$_2$) dissolved in PBLG/DMF. Such a spectrum is shown in Figure 3b. Each of the doublets in trace a is now split into two, corresponding to the two, now nonequivalent, enantiomers A and B, with splittings $\Delta\nu_Q^j$(A) and $\Delta\nu_Q^j$(B).

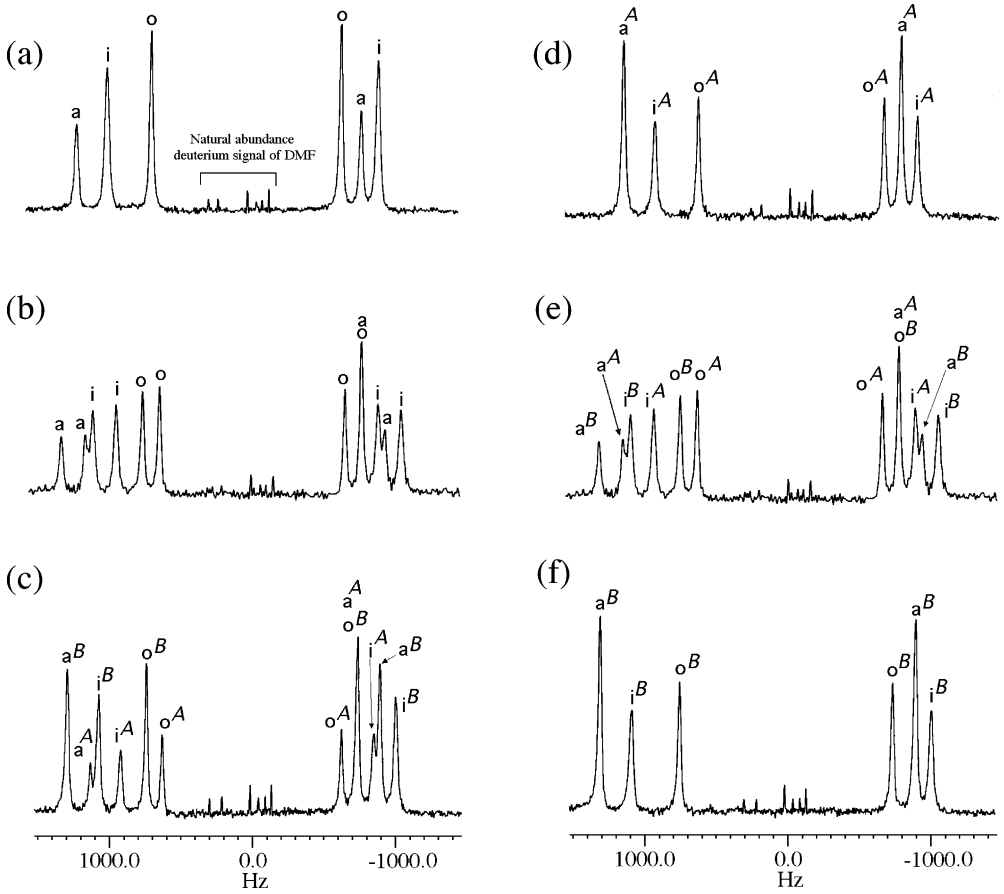

Figure 3. 61.4 MHz $^2H-\{^1H\}$ NMR spectra at $T = 320$ K of solutions of nearly equimolar mixtures of c-**1**-CD_2 and c-**1**-CD in polypeptide liquid crystals: (a) Racemic mixture of c-**1** in PBG/DMF (sample 1a). (b and e) Racemic mixture of c-**1** in PBLG/DMF (sample 2a). (c) Same solution as in part b to which an excess of enantiomer B was added (sample 3a). (d) Enantiomer A in PBLG/DMF (sample 4). (f) Enantiomer B in PBLG/DMF (sample 5). Note the signals due to natural abundant deuterons of the DMF solvent in the center region of the spectra. The total number of scans was about 3000. No filtering was applied. The center of quadrupolar doublet labeled "o" (outer deuteron) is assigned at 0 Hz.

From such a spectrum alone, no assignment of the doublets to one or the other enantiomer can be made. To do so we added to the solution of trace b a small amount of neat enantiomer B. The resulting spectrum is shown in trace c of Figure 3. The number of peaks remains the same as that in trace b, but the intensities within each pair of doublets become unequal due to the enantiomeric enrichment. This allows an unequivocal assignment of the peaks to enantiomers A and B as indicated in the figure. There are minor differences in the splittings of trace c compared to those in trace b due to slight differences in the compositions of the two solutions. For the analysis we use the results of trace b, which are the ones given in Table 3a. This table also contains similar data recorded in PBG/THF and PBLG/THF solutions. Finally, in traces d and f of Figure 3 are shown spectra of the neat enantiomers A and B in the same CLC solvent as used for traces b and c, thus confirming the above assignment. The absence of signals from a second enantiomer in these spectra indicates the high separation efficiency of the HPLC column.

A confirmation of the above assignments was obtained from a Quadrupole COrrelation SpectroscopY experiment (*Q*-COSY) 2D spectrum of deuterated c-**1** dissolved in PBLG/DMF (Figure 4a).[10−12] By applying a tilt algorithm, a 2D spectrum is obtained that allows the correlation of the components of each quadrupolar doublet with their corresponding chemical shifts in the F_2 dimension. The resulting assignment is identical to that given in Figure 3.

It is noteworthy that the quadrupole splittings for all deuterons of enantiomer B are consistently larger than those for enantiomer A in both solvents, reflecting the higher ordering of enantiomer B in both CLCs. In fact the ratio $\Delta\nu^j_Q(B)/\Delta\nu^j_Q(A)$ is essentially constant for all three doublets in a given solvent, being 1.18 in PBLG/DMF and 1.22 in PBLG/THF. This strongly suggests that the dominant chiral discrimination mechanism involves the ordering of the enantiomers. In fact, from eq 1, assuming the exact mirror-image geometry for the A and B enantiomers [$\beta^j(A) = \beta^j(B)$], it follows that $\Delta\nu^j_Q(B)/\Delta\nu^j_Q(A) = S^B_{zz}/S^A_{zz}$, independently of the deuterium site. The effect can be understood in terms of direct interaction of the solute molecules with those of the PBLG solvent, which is, of course, different for the A and B enantiomers. It will also be noted that the order parameter of the racemic solute in the achiral PBG (PBLG + PBDG) solvent is essentially equal to the average of the measured S_{zz}'s of the two enantiomers in the chiral PBLG solvent. It is as if, to the first order, the chiral interaction adds an extra term to the overall ordering of the solute, which is of opposite sign for the two enantiomers. Thus, for the order parameters of enantiomers A and B in PBLG and PBDG CLCs, we have

$$S^A_{zz}(\text{PBLG}) = S_{zz} - \Delta S/2 \qquad S^A_{zz}(\text{PBDG}) = S_{zz} + \Delta S/2 \quad (5a)$$

$$S^B_{zz}(\text{PBLG}) = S_{zz} + \Delta S/2 \qquad S^B_{zz}(\text{PBDG}) = S_{zz} - \Delta S/2 \quad (5b)$$

so that the extra ordering induced on the B enantiomer by the PBLG molecules is undone by its interaction with those of PBDG, and symmetrically the reverse sense occurs for the A enantiomer. From Table 3a, it follows that $\Delta S/S_{zz}$ is 0.16 and 0.20 for the DMF- and THF-based CLCs, where S_{zz} is the

TABLE 3: ^{2}H and ^{13}C Spectral Data for c-1 in Oriented Solvents[a]

(a) ^{2}H Data Derived from c-**1** Deuterated in the Aromatic (5a) and the Ring Methylene (7i and 7o) Sites

	δ^b/ppm			$\Delta\nu_Q{}^b$/Hz						$S_{zz} \times 10^{3\,c}$	
solvent (sample)[a]	5a	7i	7o	5a^A	5a^B	7i^A	7i^B	7o^A	7o^B	A	B
PBG/DMF (1a)	7.26	4.53	3.99	+2011		−1913		+1356		−14.1	
PBLG/DMF (2a)	7.29	4.55	3.99	−1872	+2195	−1773	−2085	+1256	+1480	−13.1	−15.4
PBG/THF(1b)	7.28	4.46	3.99	+1593		−1526		+1098		−11.2	
PBLG/THF(2b)	7.25	4.44	3.95	+1423	+1740	−1363	−1668	+980	+1198	−10.0	−12.2

(b) C5−H Couplings, $^1D_{C5-H}$ and $^1T_{C5-H}$ (in Hz) for the Crown Enantiomers Obtained from Isotopically Normal c-**1** in CLC Solutions

solvent (sample)[a]	$^1T_{C5-H}$(A)[d]	$^1T_{C5-H}$(B)[d]	$^1D_{C5-H}$(A)[e]	$^1D_{C5-H}$(B)[e]
PBG/DMF(7a)	−195		−177	
PBLG/DMF(8a)	−186	−244	−173	−202
PBG/THF(7b)	−148		−154	
PBLG/THF(8b)	−122	−164	−141	−162

(c) Magnetic Resonance Parameters for the Three Methoxy Groups of c-**1**, Derived from Natural Abundance ^{13}C and ^{2}H NMR Spectra in Liquid-Crystalline Solutions[f]

carbon site	$\delta(^2H)$/ppm	$\Delta\nu_Q$(A)/Hz	$\Delta\nu_Q$(B)/Hz	$^1T_{C-H}{}^{g,h}$/Hz	$^1D_{C-H}{}^{g,h}$/Hz
2′	3.95	+71	+96	+126	−9
3′	3.72	+470	+518	+43	−50
4′	3.77	−410	−455	+239	+47

[a] The spectra with the cosolvent DMF were recorded at 320 K, and those with THF at 300 K. [b] The accuracies of the δ and $\Delta\nu_Q$ values are around ±0.02 ppm and ±8 Hz, respectively. [c] Derived from $\Delta\nu_Q$ measured on deuteron 5a. [d] The accuracy of $^1T_{C5-H}$ values is around 5 Hz. [e] A value of $^1J_{C5-H} = +160$ Hz (Table 2b) was used in the calculations. [f] The solvent used was PBLG/DMF (samples 6 and 8a). The ^{13}C−^{1}H couplings were measured at 310 K. The quadrupolar splittings are interpolated values to 310 K from data recorded at 302 and 320 K. [g] A value of $^1J_{C-H} = +144$ Hz (Table 2b) was used in all calculations. [h] A single value is given because no, or only very small, chiral discrimination was observed in the proton-coupled ^{13}C spectrum.

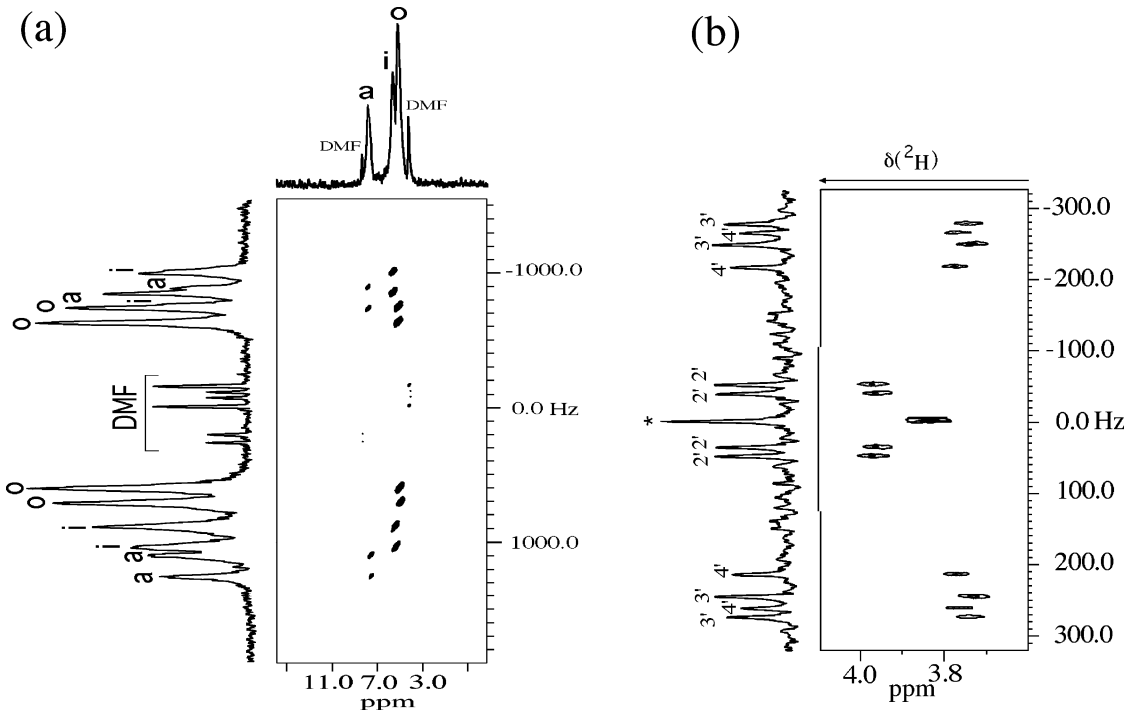

Figure 4. (a) 61.4 MHz ^{2}H−{^{1}H} *Q*-COSY 2D map of deuterated c-**1** (equal weight mixture of c-**1**-CD$_2$ and c-**1**-CD) dissolved in PBLG/DMF at $T = 320$ K (sample 2a). The Fz 2D matrix was acquired with 200 (F_1) × 2048 (F_2) data points, adding 64 scans for each transient. (b) 92.1 MHz natural abundance ^{2}H−{^{1}H} *Q*-resolved Fz 2D map of isotopically normal c-**1** dissolved in PBLG/DMF (sample 6) at $T = 320$ K. The 2D matrix was acquired with 320 (F_1) × 1440 (F_2) data points with 128 scans for each transient.

average ordering of the enantiomers. This amounts to a significant part of the overall ordering.

To conclude this section we present measurements of the natural abundant deuterons of c-**1** in the PBLG/DMF phase performed on a 14.1 T spectrometer equipped with a selective 5 mm ^{2}H cryogenic probe. These 2D experiments were recorded using the phased *Q*-resolved Fz 2D sequence.[12] In this sequence the ^{2}H chemical shifts are refocused in the t_1 dimension, while the quadrupolar interactions and the chemical shifts evolve during the acquisition time, t_2.[12] Figure 4b shows the part of the 2D map of c-**1** recorded at 320 K where the ^{2}H signals of the methoxy groups are observed. It should be noted that these ^{2}H signals correspond to a concentration of methoxy deuterated enantiomers of 14.2 μmol L^{-1} (Table 1, sample 6). The natural abundant signals of the aromatic and ring methylene deuterons (corresponding to a concentration of 4.7 μmol L^{-1}) were barely

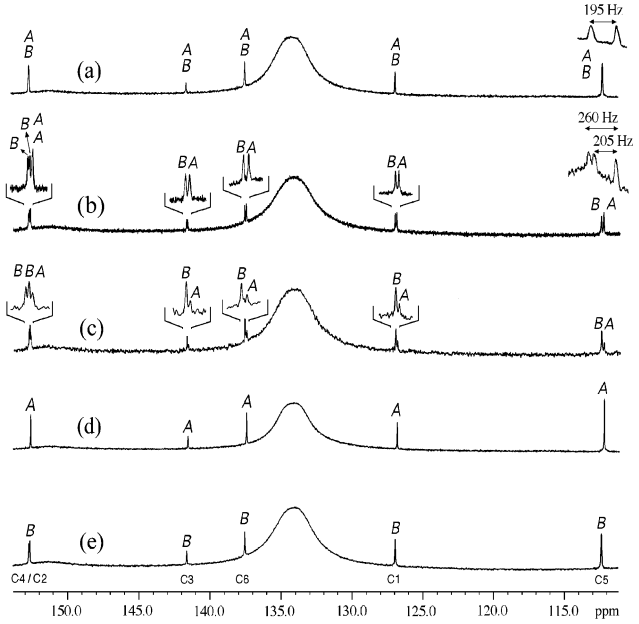

Figure 5. 100.6 MHz $^{13}C-\{^1H\}$ 1D NMR spectra of the aromatic carbons in solutions of c-**1** in polypeptide liquid-crystalline solutions at $T = 310$ K. (a) Racemic mixture of c-**1** in PBG/DMF (sample 7a). (b) Racemic mixture of c-**1** in PBLG/DMF (sample 8a). The insets above the C5 peak (in traces a and b) correspond to the same signal in the absence of proton decoupling. (c) Same solution as in part b to which an excess of enantiomer B was added (sample 9). (d) Solution of the neat enantiomer A in PBLG/DMF (sample 10). (e) Same as in part d for enantiomer B (sample 11). The broad peak at ~134 ppm is due to natural abundant aromatic ^{13}C nuclei in the polypeptide molecules. Around 10 000 scans of 16 000 data points were accumulated. No filtering window was applied.

detected due to their lower abundance and larger line widths (~20 vs ~8 Hz) compared to those of the methoxy deuterons. The 2D map in Figure 4b exhibits three pairs of doublets (centered on slightly different chemical shifts) reflecting the spectral enantio-discrimination of the three methoxy groups. A similar spectrum exhibiting somewhat larger splittings was recorded at 302 K. The results for the various δ's and corresponding $\Delta\nu_Q$'s are summarized in Table 3c. They were interpolated to 310 K from data recorded at 320 and 302 K to allow comparison with the C−H couplings, which were measured at the former temperature. The assignment of the doublets to methoxy groups 2′, 3′, and 4′ could readily be made by comparing their deuteron chemical shifts with those of the methoxy protons in Table 2a, while their assignment to enantiomers A and B was, somewhat arbitrarily, based on the results for the other deuterons in the rigid part of the molecule, for which $|\Delta\nu_Q(B)| > |\Delta\nu_Q(A)|$. Also included in Table 3c are the C−H couplings ($^1T_{C-H}$) derived from proton-coupled ^{13}C spectra of isotopically normal c-**1** in the same solvent (at 310 K). From the combined data we could determine the C−H dipolar interactions ($^1D_{C-H}$) as well as the signs of the quadrupole interactions for the three methoxy deuterons, as given in Table 3c. The assignment of the doublets with small splittings to the 2′ methoxy group and the two pairs of doublets with the larger splittings to the peripheral methoxy groups, 3′ and 4′, seems at first natural. But then it became puzzling when it turned out that the latter two have opposite signs. Clearly the diversity of the quadrupole splittings of the methoxy deuterons reflects their flexible nature. Beside the fast spinning of the methyl groups about their O−C(methyl) bonds, they can also reorient about their C(aromatic)−O bond, thus spanning a huge number of conformations. The observed splittings are averaged over all possible conformations, each with a different geometry, different abundance, and, in principle, different order parameters. The problem is thus highly underdetermined. It results in different $\Delta\nu_Q(B)/\Delta\nu_Q(A)$ ratios for the different methoxy groups (1.35, 1.10, and 1.11 for the 2′, 3′, and 4′ methoxy groups, respectively) and, as will be seen in the next section, also in solvent-dependent chiral discrimination in the ^{13}C spectra of the different methoxy carbons.

Carbon-13 NMR Spectra of the Crown Isomer in Liquid-Crystalline Solutions. We have performed a similar analysis of the natural abundance $^{13}C-\{^1H\}$ NMR spectrum of c-**1** in the polypeptide mesophases. The main effect of the ordering on such spectra is the chemical shift anisotropy (CSA) of the ^{13}C nuclei. Chiral discrimination is therefore expected to be observed predominantly for the aromatic nuclei whose CSAs are considerably larger than those of the aliphatic carbons. In trace a of Figure 5 is shown the aromatic region of the $^{13}C-\{^1H\}$ spectrum of c-**1** dissolved in an achiral PBG/DMF solution. The measured chemical shifts, including those for the aliphatic carbons (not shown), are summarized in the first row of Table 4a. The peak assignment (just above the chemical shift scale) is based on the results for the isotropic solutions (Table 2b) and some additional observations, related to carbons 2 and 4 (at 152.8 ppm), to be described below (Figure 6). Similar results for a PBG/THF solution are also included in Table 4a. It should be noted that the δ values of all aromatic carbons are consistently higher (shifted to low field) by about 1 ppm compared to their values in the isotropic solvent (Table 2b), while the shift of the aliphatic carbons is considerably smaller. This shift reflects the combined effect of ordering and CSA on the signal position in the liquid-crystalline solutions and as expected is considerably more pronounced for the aromatic carbons than that for the aliphatic carbons.

For a quantitative analysis of these shifts we recall that for a (rigid) molecule with C_3 symmetry dissolved in a liquid crystal the ^{13}C chemical shift of a particular carbon, j, is given by[15,16]

$$\delta^j = \delta^j_{iso} + S_{zz}\delta^j_{aniso} \tag{6}$$

where, (i) the anisotropy parameter is defined as

$$\delta^j_{aniso} = \frac{\delta^j_{cc}}{2}[(3\cos^2(\theta^j) - 1) - \eta^j \sin^2(\theta^j)\sin(2\varphi^j)] \tag{7}$$

(ii) the asymmetry parameter is

$$\eta^j = \frac{(\delta^j_{bb} - \delta^j_{aa})}{\delta^j_{cc}} \tag{8}$$

(iii) δ^j_{iso} is the isotropic chemical shift, and (iv) the δ^j_{kk}'s are the corresponding principal components of the (traceless) anisotropic chemical shift tensor with $\delta^j_{aa} > \delta^j_{bb} > \delta^j_{cc}$ and $\delta^j_{aa} + \delta^j_{bb} + \delta^j_{cc} = 0$. Finally, (v) the angles φ^j and θ^j are the azimuthal and polar angles of the molecular C_3 axis in the principal axis system (PAS) a^j, b^j, and c^j, of the jth carbon. As indicated above, the extra shifts due to the CSA are quite small, even for the aromatic carbons, and more importantly, there is an uncertainty in exactly estimating the δ^j_{iso}'s in our PBG solutions. Also, there may be problems related to solvent effects on the measured CSA of solutes.[17] For that reason the above data do not easily lend themselves to quantitative analysis in terms of the molecular ordering. As shown below, a more direct

TABLE 4: ^{13}C Chemical Shift Data for c-1 in Liquid-Crystalline Solutions and in the Solid State

(a) ^{13}C Chemical Shifts in Anisotropic Phase

		carbon no.									
solvent (sample)[a]		1	2	3	4	5	6	7	2′	3′	4′
PBG/DMF (7a)	δ/ppm	126.92	152.78	141.66	152.78	112.18	137.54	30.20	60.91	60.91	55.88
PBLG/DMF (8a)	δ^b/ppm	127.01	152.80	141.70	152.83	112.24	137.60	30.20	60.91	60.91	55.86
	$\Delta\nu^c$/Hz	10.3	14.4	8.5	7.2	16.8	12.5	0	0	0	4.8
PBG/THF (7b)	δ/ppm	126.89	152.88	141.96	153.02	112.16	137.59	30.46	60.80	60.70	55.82
PBLG/THF (8b)	δ^b/ppm	126.90	152.88	141.96	153.02	112.17	137.58	30.39	60.80	60.70	55.82
	$\Delta\nu^c$/Hz	8.4	10.2	6.9	7.7	14.6	10.4	0	0	~3	6.0

(b) ^{13}C Chemical Shift Tensors of the Aromatic Carbons in Solid c-**1** from MAS Experiments

	^{13}C sites					
parameters	1	2[d]	3	4[d]	5	6
δ_{iso}[e]/ppm	125.3	152.3	139.0	152.3	110.9	140.9
δ_{aa}/ppm	65.4	61.5	45.0	61.5	70	84.5
δ_{bb}/ppm	26.1	12.7	22.5	12.7	13	26.0
δ_{cc}/ppm	−91.5	−74.2	−67.5	−74.2	−83	−110.5
η[f]	0.43	0.66	0.33	0.66	0.69	0.53
δ_{aniso}[g]/ppm	−23.1	−33.8	−17.8	−16.8	−38.4	−26.5
$\nu_o\delta_{aniso} \times 10^{-3}$/Hz	−2.32	−3.40	−1.79	−1.69	−3.86	−2.67

[a] Solutions with DMF as the cosolvent were measured at 310 K, and those with THF at 300 K. [b] Average value if chiral discrimination is observed. [c] Chiral discrimination, $\Delta\nu = \nu^B - \nu^A = \nu_o(\delta^B - \delta^A)$ for $\nu_o = 100.6$ MHz. [d] Since the peaks due to carbons 2 and 4 overlapped, a common tensor was assumed for both. [e] Weighted average when a multiplet band was observed. [f] See eq 8. [g] Calculated using eq 7, with $\theta^j = 43°$ for all aromatic carbons, and $|\varphi^j|$ equals, respectively, 90°, 150°, and 30° for j = (2 and 5), (1 and 6), and (3 and 4).

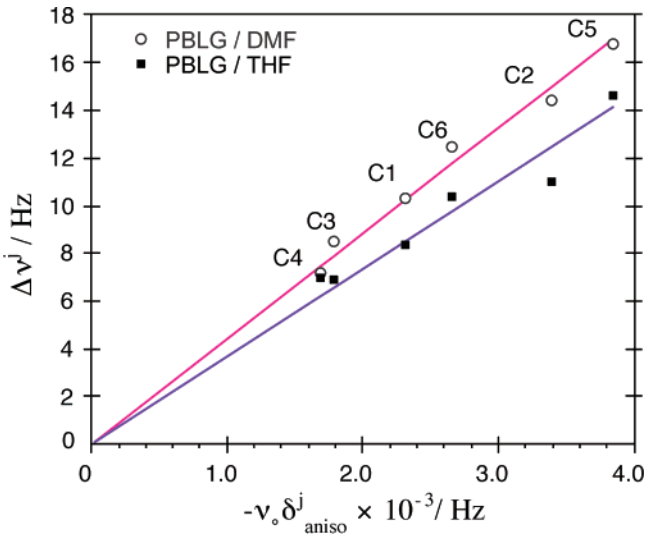

Figure 6. Plots of the chiral discrimination, $\Delta\nu^j = \nu^j(B) - \nu^j(A)$, of the aromatic carbons of c-**1** vs the anisotropy parameter, δ^j_{aniso}, for the two CLCs, PBLG/DMF (sample 8a) and PBLG/THF (sample 8b). $\Delta\nu^j$ and δ^j_{aniso} were derived from Tables 4a and 4b, respectively. The "C_n" notation on the graphs labels the six aromatic carbons (Figure 1).

way to do so is using the chiral discrimination in the CLC solutions. By taking the differences of the observed chemical shifts of the two enantiomers the problems related to the solvent effect on the δ^j_{aniso}'s and the choice of the δ^j_{iso}'s are largely eliminated.

In trace b of Figure 5 is shown a ^{13}C−{^{1}H} spectrum for a solution of c-**1** in PBLG/DMF. Each of the aromatic peaks is now doubled, thus reflecting the chiral discrimination between the A and B enantiomers. The assignment of the peaks to one or the other enantiomers can readily be made on the basis of trace c of Figure 5, which corresponds to a solution of c-**1**, containing an excess of enantiomer B (B/A ratio ≈ 3). The number of peaks in this spectrum is the same as in trace b of Figure 5, but the doublets are now asymmetric in their intensity, allowing direct assignment of the peaks, as indicated in the figure. The average chemical shifts (in ppm), $[\delta^j(A) + \delta^j(B)]/2$, and the chiral separation (frequency differences in Hz), $\Delta\nu^j = [\nu^j(B) - \nu^j(A)] = \nu_o[\delta^j(B) - \delta^j(A)]$ (where ν_o is the ^{13}C Larmor frequency), are summarized in the second and third rows of Table 4a. Similar data for the PBLG/THF solution are given in rows 5 and 6 of the table. It should be noted that the signals of enantiomer B are always shifted to lower field ($\Delta\nu^j$ positive), reflecting the fact that the (magnitude of the) ordering of enantiomer B is higher than that of A, as was also found from the ^{2}H spectra. Note several additional entries in Figure 5. These include expanded spectral regions demonstrating the chiral discrimination of the various peaks as well as insets of un-decoupled spectra of the C5 carbon in both the achiral (trace a) and the chiral (trace b) liquid-crystalline solutions, which exhibit splittings due to the ^{13}C5−^{1}H interaction, $^1T_{C5-H}$. These results as well as similar data for the methoxy carbons are included in Tables 3b and 3c and have been discussed above in connection with the analysis of the deuterium spectra. Finally we show in the two bottom traces of Figure 5 examples of spectra of the neat enantiomers A and B in a PBLG/DMF solution. These spectra demonstrate the high efficiency of the chromatographic separation of enantiomers as also noted for the deuterated compounds.

The chiral discrimination in the ^{13}C spectrum can be explained in much the same way as that for the ^{2}H spectrum in terms of a slight difference in the ordering of the two enantiomers when dissolved in a CLC. From eqs 5−8, the chiral discrimination of the various carbons is given by

$$\Delta\nu^j = \nu^j(B) - \nu^j(A) = \nu_o[\delta^j(B) - \delta^j(A)] = \nu_o(S^B_{zz} - S^A_{zz})\delta^j_{aniso} = (\Delta S)(\nu_o\delta^j_{aniso}) \quad (9)$$

It follows that a plot of the chiral discrimination, $\Delta\nu^j$, of the various carbons versus $\nu_o\delta^j_{aniso}$ should give a straight line passing through the origin with a slope equal to ΔS. To check this relationship we have determined the full anisotropic tensors of the aromatic carbons of c-**1** by analyzing their spinning side bands in the MAS spectrum of a solid sample. Measurements

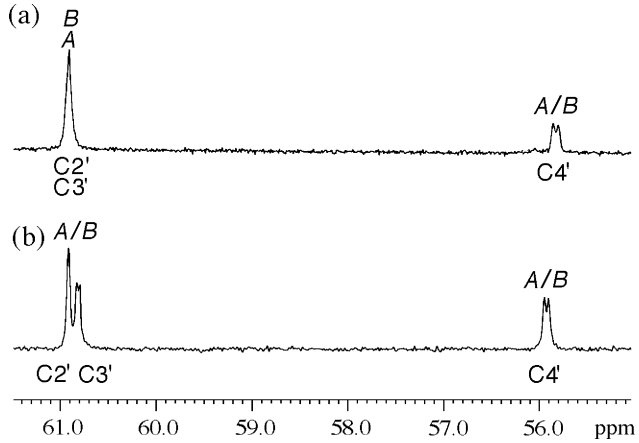

Figure 7. Examples of 100.6 MHz $^{13}C-\{^1H\}$ NMR spectra in the aliphatic region for a racemic solution of c-**1** in (a) PBLG/DMF (T = 310 K, sample 8a) and (b) PBLG/THF (T = 300 K, sample 8b).

were carried out at several spinning rates, and the spectra were analyzed by the Herzfeld−Berger method.[18] The results are summarized in Table 4b. From these results, using eq 7, we have calculated the $\delta_{aniso}{}^j$'s (and $\nu_o\delta_{aniso}{}^j$'s) for the various aromatic carbons as given in the last two lines of Table 4b. For these calculations we have assumed that for all of the (aromatic) carbons the most shielded principal chemical shift tensor component, δ_{cc}, lies normal to the benzene ring and that the least shielded component, δ_{aa}, lies along the ring radial direction. Also, from the known geometry of the CTV core,[19] we used $\theta^j = 43°$ for all carbons, while $|\varphi^j|$ was taken as 90°, 150°, and 30° for, respectively, j = (2 and 5), (1 and 6), and (3 and 4). Using these data we finally plot in Figure 6 the measured $\Delta\nu^j$ values for the various aromatic carbons in the two CLC solutions (PBLG/DMF and PBLG/THF) against the $\nu_o\delta_{aniso}{}^j$ values so obtained. Good linear relations are observed for both solutions, yielding ΔS values of -3.7×10^{-3} and -4.4×10^{-3} for the two CLC solutions, respectively. The negative sign of ΔS follows from the fact that $|S_{zz}^B| > |S_{zz}^A|$, and the sign of the S_{zz}'s is negative. These values are consistent with those derived from the deuterium spectra and confirm that the dominant factor influencing the chiral discrimination in the NMR spectra is the different ordering of the enantiomers in the CLCs.

A comment about the assignment of the ^{13}C signals of carbons C2 and C4 is in order at this point. It will be recalled that in solution the signals of these carbons fall very close to each other (and in the MAS spectrum they are unresolved). Their assignment in the solution spectra (required to determine their $\Delta\nu^j$ values) is thus problematic and carried out as follows. In CLC these carbons exhibit four lines, two pairs of chiral doublets, C2(A), C2(B), C4(A), and C4(B). They can be analyzed in terms of three possible pairs of chiral discriminations. We have chosen the particular pairing so that their $\Delta\nu^j$'s would best fit the straight lines in Figure 6. The larger of the two splittings was assigned to C2 (because of its larger $|\delta_{aniso}^j|$), and the smaller to C4. The remaining deviation of the points due to C2 from the straight lines is ascribed to the relatively larger uncertainty in its δ_{aniso}^j value. Since the signals of C2 and C4 overlap in the solid state, we analyzed their MAS spectrum in terms of a common chemical shift tensor. This is clearly a gross approximation.

We conclude this discussion of the ^{13}C spectra of the crown isomer by commenting on the signals due to the methoxy groups. Examples of spectra in the CLC solvents, PBLG/DMF and PBLG/THF (with the peak assignment), are shown in, respectively, traces a and b of Figure 7. The corresponding chemical shifts (also for the corresponding achiral PBG solutions) are included in Table 4a. Two main points may be made in connection with these spectra. First, while the peaks of C2′ and C3′ are resolved in the THF liquid-crystalline solution, they are not resolved in the DMF one. This difference is most likely due to a solvent effect on the conformational distribution of the side chains. The second point concerns the clearly resolved chiral discrimination in the signals due to C4′ in spectrum a and C3′ and C4′ in spectrum b. In fact the observed splittings are not much smaller than those observed for the aromatic carbons, even though these carbons have much smaller δ_{aniso}'s and they are associated with smaller effective order parameters. This somewhat larger than expected chiral discrimination may also be due to the effect of the conformational distribution of the methoxy groups. In particular, the conformational distribution may be different for the two isomers in the CLCs. A quantitative analysis of this effect is complicated by the fact that due to the large number of possible conformations the problem is highly underdetermined.

^{13}C and ^2H NMR Spectra of the Saddle Isomer in Liquid-Crystalline Solutions. As indicated in the Introduction the "frozen" saddle isomer, with C_1 symmetry (Figure 1b), is chiral. It cannot, however, be separated into its enantiomers because in solution (and in the melt) this isomer undergoes fast pseudorotation that interconverts its various conformers. The rate of this process is so fast that it cannot be frozen out (on the NMR time scale) even by cooling down to very low temperatures. This was demonstrated for the hexamethoxy derivative, which showed no line-broadening due to slowing down of this process, even by cooling down to 100 K.[8] Consequently, no chiral discrimination between enantiomers can be observed in the NMR spectrum of s-**1** in chiral solvents, as was observed for the crown isomer. Its solution ^1H and ^{13}C NMR spectra (Figure 2) with, respectively, a single aromatic (5), single methylene (7), and three methoxy (2′, 3′, and 4′) ^1H peaks, and six aromatic (1−6), a single methylene, and three methoxy ^{13}C peaks, are entirely consistent with fast pseudorotation.

The "average" structure of the rapidly pseudorotating saddle isomer is planar with a 3-fold rotation symmetry. It corresponds to the symmetry point group C_{3h} with all nuclei of the TBCN core lying in the average symmetry plane except for the ring methylene hydrogens, which are symmetrically positioned below and above this plane. The molecule is thus achiral, but the methylene C−H bonds are enantiotopic and in chiral media may exhibit spectral enantio-discrimination. In Figure 8 is shown the ^{13}C spectrum of s-**1** in a PBLG/DMF solvent. The spectrum is well-resolved, showing a single peak for each type of carbon with, as expected, no indication of peak doubling. The spectral data are essentially identical to those measured in the achiral PBG/DMF solvent, as can be verified from Table 5a. They are in fact also very similar to those of s-**1** dissolved in an isotropic DMF solution (Table 2b). However the $^2H-\{^1H\}$ spectrum of deuterated s-**1** (equimolar mixture of s-**1**-CD_2 and s-**1**-CD) shows a different behavior in the achiral and chiral liquid-crystalline solvents (Figure 9). In the achiral solvent (trace a) there is a single doublet for the aromatic as well as for the methylene deuterons, while in the chiral solvent (trace b) the latter is split into a pair of doublets, reflecting the nonequivalence of the enantiotopic methylene deuterons in a CLC solution. The numerical data for the deuterium spectra are given in Table 5b. For completion we include in Table 5c the $^1T_{C-H}$ couplings for the aromatic (5) and ring methylene (7) C−H pairs and the corresponding average dipolar couplings, $^1D_{C-H}$, measured in isotopically normal s-**1**. These were derived from proton-coupled

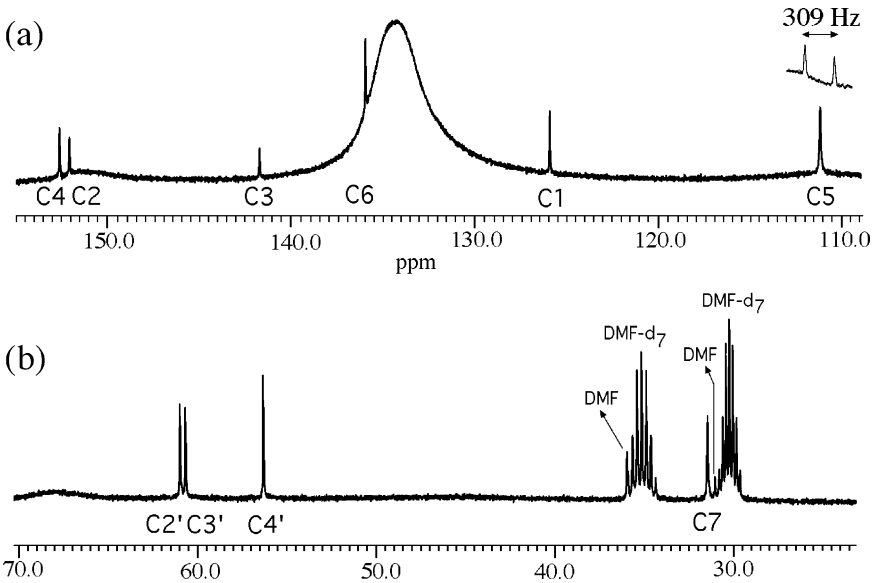

Figure 8. 100.6 MHz $^{13}C-\{^1H\}$ NMR spectra with the peak assignment of s-**1** in the chiral PBLG/DMF mesophase (sample 13a). (a) Aromatic region of the spectrum at $T = 310$ K. The inset for C-5 is the proton-coupled spectrum. (b) As in part a for the aliphatic region. In addition to the methoxy and ring methylene carbons, the peaks due to deuterated and isotopically normal DMF cosolvent are indicated.

TABLE 5: ^{13}C and ^2H Magnetic Resonance Parameters for s-1 in Oriented Solvents

(a) ^{13}C Chemical Shifts (in ppm)

	^{13}C notation									
solvent (sample)[a]	1	2	3	4	5	6	7	2′	3′	4′
PBG/DMF (12a)	125.96	152.27	141.81	152.78	111.25	135.99	31.48	61.03	60.75	56.35
PBLG/DMF (13a)	125.99	152.26	141.83	152.80	111.24	136.04	31.45	61.04	60.73	56.35
PBG/THF (12b)	126.11	152.60	142.24	153.01	111.24	136.27	31.93	60.94	60.60	56.27
PBLG/THF (13b)	126.13	152.62	142.26	153.03	111.26	136.29	31.93	60.94	60.61	56.27

(b) Deuterium Chemical Shifts and Quadrupolar Splittings for the Aromatic (5), and Ring Methylene (7) Deuterons[b,c]

	^2H sites			
	5		7	
solvent (sample)	δ^d/ppm	$\Delta\nu_Q{}^d$/Hz	δ^d/ppm	$\Delta\nu_Q{}^d$/Hz
PBG/DMF (14a)	6.60	−705	3.92	−661
PBLG/DMF (15a)	6.60	−671	3.92	−594/−652
PBG/THF (14b)	6.61	−628	3.92	−462
PBLG/THF (15b)	6.61	−617	3.92	−416/−490

(c) C5−H and C7−H Couplings (in Hz) from ^{13}C Spectra of Isotopically Normal s-**1**[a]

solvent (sample)	$^1T_{C5-H}{}^e$	$^1D_{C5-H}{}^{e,f}$	$^1T_{C7-H}{}^e$	$^1D_{C7-H}{}^{e,f}$
PBG/DMF (12a)	+291	+67	+246	+59
PBLG/DMF (13a)	+291	+67	+246	+59
PBG/THF (12b)	+283	+63	+222	+47
PBLG/THF (13b)	+289	+66	+226	+49

[a] Solutions with DMF as the cosolvent were measured at 310 K, and those with THF at 300 K. [b] The solute consisted of a mixture of the s-**1**-CD_2 and s-**1**-CD isotopomers. [c] The measurements in DMF were done at 320 K, and those in THF at 300 K. [d] The accuracies of the δ and $\Delta\nu_Q$ values are around ±0.02 ppm and ±8 Hz, respectively. [e] The accuracy of $^1T_{C-H}$ values is around ±5 Hz. [f] For the calculation, values of $^1J_{C5-H} = +157$ Hz and $^1J_{C7-H} = +128$ Hz, as measured in isotropic solutions, were used.

^{13}C spectra (see inset for C5 in Figure 8) and were used to determine the signs of the dipolar and quadrupolar interactions of these C−H(D) pairs, as described previously.

The spectral discrimination observed for the C−D enantiotopic directions is consistent with the basic principles of chirality and should therefore not be surprising. The symmetry of the "average" saddle isomer, when dissolved in a CLC reduces from C_{3h} to C_3, rendering the pairs of enantiotopic methylene deuterons nonequivalent. Yet, such discrimination is in general not observed for rigid molecules possessing a C_n symmetry axis ($n \geq 3$). This lack of discrimination, for rigid molecules, is based on the notion that the dominant factor influencing chiral discrimination in CLC is the ordering of the solute. Rigid molecules with a C_n symmetry axis ($n \geq 3$) dissolved in a uniaxial liquid-crystalline phase are characterized by an axial ordering tensor with a single independent order parameter, S_{zz}. This situation is not changed when the solute is dissolved in a CLC.[20] Consequently, unless the geometry of the solute molecule or its electronic structure is significantly distorted by the chiral environment (so that the magnetic parameters of symmetrically positioned atoms become dissimilar), the degeneracy of its enantiotopic groups is not lifted. Solute−solvent interactions are usually too weak to produce such distortions, and hence no spectral discrimination of

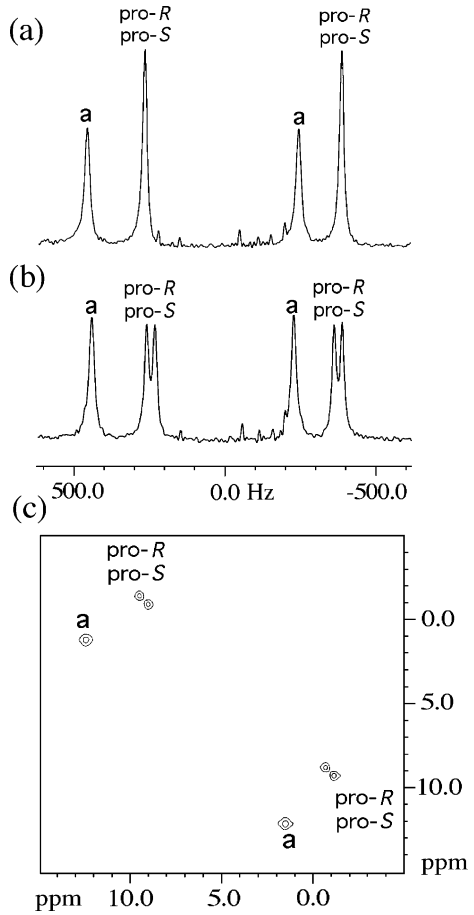

Figure 9. 61.4 MHz ^{2}H−{^{1}H} 1D NMR spectra of an equal mass mixture of the saddle isotopomers, s-**1**-CD$_2$ and s-**1**-CD (T = 320 K). (a) Dissolved in the achiral mesophase, PBG/DMF, (sample 14a). (b) Dissolved in the chiral mesophase, PBLG/DMF, (sample 15a). (c) ^{2}H−{^{1}H} *Q*-COSY 2D map of the same solution as in part b. The 2D matrix was acquired with 320 (F_1) × 1500 (F_2) data points, and 32 scans were added for each transient.

enantiotopic groups is observed for rigid uniaxial solutes.[1] For example in CLC solutions of the parent crown compound, CTV (hexamethoxy-TBCN) with C_{3v} symmetry, no chiral discrimination was observed in neither the ^{13}C nor the ^{2}H spectra of atoms or groups of atoms related by the vertical reflection planes of the molecule. However, when the CTV core was symmetrically substituted with flexible dioxyethylene groups (still with an average C_{3v} symmetry), the latter did exhibit such a discrimination.[1] The observation of enantiotopic discrimination in the NMR spectra of flexible solutes (with an average C_3 symmetry axis) must therefore be related to the conformational interconversion between chiral conformers with different molecular ordering. This in turn may lead to chiral discrimination of sites that on the average are enantiotopically related. In other words, in uniaxial, flexible solutes the spectral discrimination of internuclear directions, which on the average are enantiotopic, results from the discrimination of chiral conformers in the course of the conformational dynamics. In the next section we discuss in detail the case of s-**1** and perform a quantitative analysis of the factors leading to the observed enantiotopic discrimination in this compound.

Analysis of the Pseudorotation and the Origin of the Enantiotopic Discrimination in s-1. To understand the origin of the chiral discrimination of the NMR signals due to the methylene deuterons of s-**1** in the CLC, we calculate their average $\Delta\nu_Q$ over the pseudorotation cycle. In Figure 10 are shown the various conformations that comprise the pseudorotation cycle. There are six such conformers differing from each other by cyclically moving one of the benzene rings up or down relative to the others (without the whole molecule performing an actual rotation). The cycle is also shown in the scheme below, where the Roman numbers label the conformer and "u" (up) and "d" (down) indicate the relative orientation of the benzene rings (labeled clockwise 1, 2, and 3) as in Figure 10.

$$\leftrightarrow \underset{\text{I}}{(u,d,d)} \leftrightarrow \underset{\text{II}}{(u,d,u)} \leftrightarrow \underset{\text{III}}{(d,d,u)} \leftrightarrow \underset{\text{IV}}{(d,u,u)} \leftrightarrow \underset{\text{V}}{(d,u,d)} \leftrightarrow \underset{\text{VI}}{(u,u,d)} \leftrightarrow \quad (10)$$

It will be noticed that the six conformers consist of three pairs of enantiomers (I and IV; III and VI; and V and II). The superimposable homomers I, III, and V comprise one enantiomer, to be labeled B, while the homomers II, IV, and VI comprise enantiomer C. The structures of these enantiomers are shown on the left (conformer I) and right (conformer IV) sides of Figure 1b. It may also be noted in Figure 10 that the various conformers of the saddle isomer can be generated from each other by operations isomorphic with those of the symmetry group, C_{3h}. These comprise the isodynamic group referred to in the Introduction when discussing the "average symmetry" of the saddle isomer.[9] To calculate the average deuterium quadrupole interaction of the methylene deuterons, we need to follow their "history" over the pseudorotation cycle. To do so we label the methylene deuterons with two indices, one for indicating the methylene groups and the other for distinguishing between the enantiotopic sites within the methylene groups. These indices are independent of the conformation. The methylene groups are labeled according to the numbering of the oppositely lying benzene rings (methylene-1, -2, or -3), while the enantiotopic deuterons within a methylene group are distinguished by using the stereodescriptors *pro-R* and *pro-S*.[21] Moving clockwise around the outer periphery of the cyclononatriene ring the *pro-R* (*pro-S*) direction is obtained by clockwise (anticlockwise) rotation of the methylene bisector by half of the methylene bond angle. In practice we labeled the *pro-R* and *pro-S* deuterons in conformer I, which we used as a reference. As the conformers are either homomers or enantiomers the labeling of the enantiotopic sites in the other conformers could readily be obtained by, respectively, rotation or reflection. In Figure 10, the *pro-R* and *pro-S* deuterons are colored in green and blue, respectively. To identify the molecular sites for the purpose of calculating the quadrupole coupling in each conformer, we again use conformer I as a reference. As shown in Figure 1b (left) the sites occupied by the *pro-R* and *pro-S* deuterons, in this conformer, are labeled "b" and "c", respectively (reserving the letter "a" for the aromatic deuteron). We further label the sites by the methylene numbers, as above, as well as by the superscript B (or C for the second enantiomer) as a reminder of the conformer's configuration. Thus, in the reference conformer I, $(b1)^B$ corresponds to the site of the inner methylene deuteron, opposite benzene ring "1", etc.

During the pseudorotation cycle the methylene deuterons change their stereochemical environment. Thus, in conformation II the deuteron *pro-R* (methylene-1), originally in site $(b1)^B$, occupies site $(c3)^C$, where the superscript reminds us that this conformer is a C enantiomer. Likewise, the *pro-S* (methylene-1) deuteron, originally in site $(c1)^B$, occupies in conformer II the site $(b3)^C$, and the *pro-R* (methylene-2) deuteron, $(b2)^B$, moves to site $(c1)^C$, etc. The whole occupation history over the full pseudorotation cycle is summarized in Table 6, where for

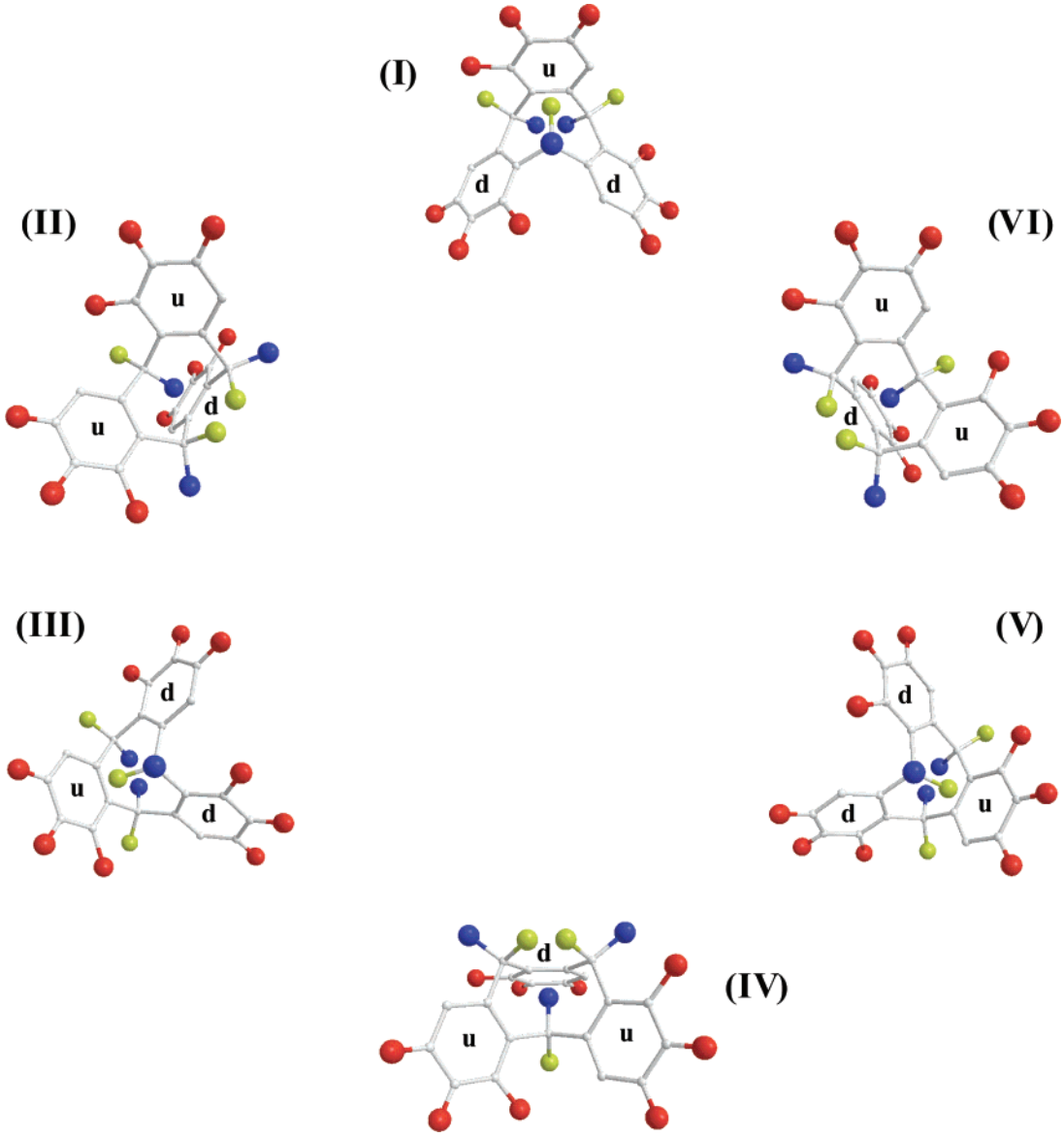

Figure 10. Schematic representation of the pseudorotation cycle of the saddle isomer, s-**1**. The red spheres represent methoxy groups. The green and blue spheres represent, respectively, the *pro-R* and *pro-S* methylene deuterons in each conformer. The aromatic deuterons are not displayed. The Roman letters label the conformers as in eq 10. The letters "u" and "d" inside (or next to) the benzene rings indicate their orientations relative to each other. All conformers are represented with benzene ring 1 over rings 2 and 3 and ring 2 on the right of ring 3. Note that conformers I, III, and V are homomers and likewise conformers II, IV, and VI and the two sets are enantiomerically related. Conformer I corresponds to the left structure of Figure 1b, while conformer IV corresponds to the right one rotated by 180° about a vertical axis.

TABLE 6: Six Pseudorotating Conformers of the Saddle Isomer of 1[a]

conformer[b]	ring orientations of rings 1, 2, and 3[c]	enantiomer B/C[d]	methylene-1[e]		methylene-2[e]		methylene-3[e]	
			pro-R [f]	*pro-S* [f]	*pro-R* [f]	*pro-S* [f]	*pro-R* [f]	*pro-S* [f]
I	u d d	B	b1	c1	b2	c2	b3	c3
II	u d u	C	c3	b3	c1	b1	c2	b2
III	d d u	B	b2	c2	b3	c3	b1	c1
IV	d u u	C	c1	b1	c2	b2	c3	b3
V	d u d	B	b3	c3	b1	c1	b2	c2
VI	u u d	C	c2	b2	c3	b3	c1	b1

[a] The entries in columns 4−9 indicate the stereochemical positions occupied by the methylene deuterium atoms in the various conformers. [b] Labeling of conformers. [c] Relative positions of the benzene rings 1, 2, and 3. [d] Identification of enantiomers. [e] Numbering of the methylene groups according to the oppositely lying benzene rings. [f] Stereochemical descriptors of enantiotopic methylene deuterons. These descriptors are not defined for a particular conformer.

simplicity the superscripts labeling the enantiomers are given separately in the third column. In checking the table, remember that the C and B enantiomers are related to each other by a reflection, as shown in Figure 1b. We also note that in an achiral environment the six $(pj)^{B}$ sites are equivalent to the corresponding $(pj)^{C}$ sites (p = b or c; j = 1, 2, or 3), but in chiral solvents they may differ.

Several regularities may be noted in Table 6. In particular we note that the *pro-R* and *pro-S* deuterons, namely, deuterons that in the reference conformer (I) occupy, respectively, a "b"

or a "c" site, do not have exactly the same history. A *pro-R* deuteron will occupy b sites only in B conformers and c sites only in C conformers. Conversely, a *pro-S* deuteron will only occupy a "b" site in C conformers and a "c" site in B conformers. Thus during a complete pseudorotation cycle (see Table 6), a *pro-R* deuteron will visit the sites $(b1)^B$, $(c3)^C$, $(b2)^B$, $(c1)^C$, $(b3)^B$, and $(c2)^C$, while a *pro-S* deuteron will visit the sites $(c1)^B$, $(b3)^C$, $(c2)^B$, $(b1)^C$, $(c3)^B$, and $(b2)^C$ with different orders, depending on its original site (in the I conformer). In achiral liquid crystals, where the abundance and ordering of all conformers are the same, the exchange-averaged quadrupolar splittings for the *pro-R* and *pro-S* deuterons become, respectively

$$\langle \Delta\nu \rangle^{pro\text{-}R} = \frac{1}{2}[\langle \Delta\nu_Q^b \rangle^B + \langle \Delta\nu_Q^c \rangle^C] \quad (11a)$$

$$\langle \Delta\nu \rangle^{pro\text{-}S} = \frac{1}{2}[\langle \Delta\nu_Q^c \rangle^B + \langle \Delta\nu_Q^b \rangle^C] \quad (11b)$$

where the $\langle \Delta\nu_Q^p \rangle^K$'s are the average splittings of the *p*-type deuterons (p = b, c) in the *K*th enantiomer (K = B, C) over the three methylene sites, j = 1, 2, or 3

$$\langle \Delta\nu_Q^p \rangle^K = \frac{1}{3}[\langle \Delta\nu_Q^{p1} \rangle^K + \langle \Delta\nu_Q^{p2} \rangle^K + \langle \Delta\nu_Q^{p3} \rangle^K] \quad (12)$$

and the $\langle \Delta\nu_Q^{pj} \rangle^K$'s are the motionally averaged deuterium quadrupole interactions in the *pj* sites of the *K* enantiomer. The expressions for the $\langle \Delta\nu_Q^{pj} \rangle^K$'s are complicated due to the low symmetry (C_1) of the saddle isomer, requiring five independent motional constants to describe its average orientation in a liquid crystal solution.[22] One might naively think that the fast interconversion (on the NMR time scale) between the structurally equivalent saddle conformers (which results in an average spin Hamiltonian with axial symmetry) will alleviate this difficulty. However, as discussed by several authors in the past, this is not the case, and an exact analysis still requires five motional constants.[23−26] These constants can be thought to consist of three Euler angles, describing the molecular fixed coordinate system (*X*, *Y*, and *Z*) in which the ordering matrix is diagonal, and two additional terms, S_{zz} and $(S_{xx} - S_{yy})$, corresponding to the axial and rhombic order parameters, respectively. Without loss of generality (and since we do not intend to perform numerical analyses of the results) we may assume that the X^K, Y^K, and Z^K directions in the molecular frame of the saddle isomers are known. In these systems, $\langle \Delta\nu_Q^{pj} \rangle^K$'s are given by

$$\langle \Delta\nu_Q^{pj} \rangle^K = \left(\frac{3}{2}\right) Q_{C-D} S_{zz}^K \left\{ \left(\frac{1}{2}\right)[3\cos^2(\beta_z^{pj})^K - 1] + \left(\frac{1}{2}\right)\epsilon^K [\cos^2(\beta_x^{pj})^K - \cos^2(\beta_y^{pj})^K] \right\} \quad (13)$$

where $\epsilon^K = (S_{xx}^K - S_{yy}^K)/S_{zz}^K$ and $S_{\gamma\gamma}^K$are the diagonal motional constants, $(\beta_\gamma^{pj})^K$ are the angles between the C−D^{pj} bond and the γ-principal ordering axes in the *K*th enantiomer, and we retained the assumption of an axial deuterium quadrupole tensor. Clearly in achiral solvents, the principal ordering frames in the two enantiomers are related by reflection (as do the enantiomers themselves), and $S_{\gamma\gamma}^B = S_{\gamma\gamma}^C$ for all γ's. Consequently, $\langle \Delta\nu_Q^b \rangle^B = \langle \Delta\nu_Q^b \rangle^C = \langle \Delta\nu_Q^b \rangle$ and $\langle \Delta\nu_Q^c \rangle^B = \langle \Delta\nu_Q^c \rangle^C = \langle \Delta\nu_Q^c \rangle$. Hence, from eqs 11−13

$$\langle \Delta\nu_Q \rangle^{pro\text{-}R} = \langle \Delta\nu_Q \rangle^{pro\text{-}S} = \frac{1}{2}[\langle \Delta\nu_Q^b \rangle + \langle \Delta\nu_Q^c \rangle] \quad (14)$$

and only a single doublet is observed for the methylene deuterons (Figure 9a).

The situation is different in CLCs. In such solvents, parameters associated with the B and C enantiomers need not be identical. For example, their equilibrium populations, P^B and P^C, the magnetic parameters of corresponding sites, $\langle \Delta\nu_Q^{pj} \rangle^B$ and $\langle \Delta\nu_Q^{pj} \rangle^C$, and in particular the principal directions (γ^K) and magnitudes ($S_{\gamma\gamma}^K$) of the ordering tensor may differ in the B and C enantiomers. Consequently the average quadrupole interactions of the *pro-R* and *pro-S* deuterons will in general be different, resulting in chiral discrimination, as observed experimentally (Figure 9b). In practice the effect of solvent chirality on the equilibrium concentration of the enantiomers is not likely to be important, and we may assume that $P^B = P^C = {}^1/_2$.[27] From eq 11 we then obtain

$$\Delta\Delta\nu_Q = \langle \Delta\nu_Q \rangle^{pro\text{-}R} - \langle \Delta\nu_Q \rangle^{pro\text{-}S} = \frac{1}{2}[(\langle \Delta\nu_Q^b \rangle^B + \langle \Delta\nu_Q^b \rangle^C) - (\langle \Delta\nu_Q^c \rangle^B + \langle \Delta\nu_Q^c \rangle^C)] \quad (15)$$

The discrimination thus reflects the differences in the average splittings of deuterons b and c in the two enantiomers. These differences vanish, of course, in achiral solvents. In view of the many unknown parameters in eq 15, the problem is highly underdetermined, leaving not much hope for a quantitative analysis of the results. Nevertheless, to obtain a physical "feeling" for the origin of the discrimination let us assume that the rhombic terms in the $\langle \Delta\nu_Q^p \rangle^K$'s are small compared to the corresponding axial ones (a situation that often occurs in reality) and that the geometry of the enantiomers is not affected by the chiral environment (β_z^{pj} independent of *K*). The chiral discrimination then assumes the form

$$\Delta\Delta\nu_Q = \frac{1}{2}[(S_{zz}^B - S_{zz}^C)(\sum{}^b - \sum{}^c)] \quad (16)$$

where

$$\sum{}^p = \left(\frac{3}{2}\right) Q_{C-D} \left(\frac{1}{3}\right) \sum_{j=1,2,3} [3\cos^2(\beta_z^{pj}) - 1]/2 \quad (17)$$

In this approximation, two factors determine $\Delta\Delta\nu_Q$ of the exchange-averaged enantiotopic deuterons in s-**1**, the difference of the ordering of the two types of enantiomers involved in the pseudorotation cycle and the difference in the mean quadrupole interactions of the deuterons in the sites b and c, none of which can be determined independently. The complexity of the problem is further augmented by the fact that we have no way to identify the two doublets with the *pro-R* and *pro-S* deuterons. In a randomly deuterated sample their relative intensities are always 1:1 (independent of the relative populations P^B/P^C), and it is difficult to imagine a synthetic route leading to a specific labeling of a particular site.

It should be noted that eqs 15 and 16 hold for the fast exchange limit of NMR, namely, when the inverse lifetime of the enantiomers is larger than the differences in the $\langle \Delta\nu_Q^{pj} \rangle$'s. At the same time the lifetime of the conformers should also be longer than their rotational correlation time, so a well-defined ordering is established for the enantiomers. This sets an upper limit for the pseudorotation rate on the order of the molecular reorientation time. For very fast pseudorotation processes (faster than the molecular reorientation), an average order parameter for the "average" molecule is established, and no chiral

discrimination is expected. This situation clearly does not apply in the present work.

A similar analysis can be made for the aromatic deuterons (labeled a). It may, however, readily be confirmed (Figure 10) that during a pseudorotation cycle these deuterons visit all six $(aj)^K$ sites. Consequently, a single doublet with an average splitting is obtained in both achiral and chiral solvents, and no chiral discrimination is expected (nor observed). In this connection it is interesting to compare the results for D_{C5-H} and $\Delta\nu_Q{}^5$ in the saddle and crown isomers (Tables 3 and 5). It will be noted that the magnitudes of these parameters in the saddle isomer are about one-third of those in the crown isomer and of the opposite sign. These differences reflect the delicate dependence of these parameters on the structure and dynamics of the saddle conformer, as discussed above.

Summary and Conclusions

We have presented ^{13}C and ^{2}H NMR spectra of the two isomers of **1** dissolved in achiral and chiral PBG-based mesophases. The crown isomer is rigid and possesses structural chirality. Its racemic mixture in chiral solvents exhibits doubling of the NMR spectrum, reflecting the nonequivalence of its enantiomers in chiral oriented environments. It is shown that for the carbon-13 and deuterium spectra the chiral discrimination is proportional to, respectively, the average CSA and the quadrupolar splitting of the two enantiomers. This strongly indicates that the chiral discrimination is predominantly due to the different ordering of the two enantiomers. The spectra of the racemic mixture were compared with those of the neat enantiomers obtained by chiral HPLC separation. This allowed identification of the enantiomers according to the relative degree of ordering. If this relative ordering could be calculated or determined by some kind of a semiempirical method, then such chiral discrimination could be used to determine the absolute conformation of optical isomers. So far no such reliable methods were developed.

The saddle isomer is highly flexible, undergoing rapid interconversion between several (chiral) conformations. It has an "average" planar geometry (with C_{3h} symmetry) and is therefore achiral. The ring methylene deuterons are, however, enantiotopically related, and their ^{2}H spectrum in chiral solvents exhibits chiral discrimination. Such discrimination of enantiotopic sites is generally not observed in rigid prochiral molecules possessing a C_n symmetry axis ($n \geq 3$), although it is apparently common in flexible molecules with similar average symmetries. We show that the chiral discrimination in the latter results from the different ordering of the chiral conformers during the interconversion cycle, which differently affect the enantiotopic sites. A quantitative expression is derived for the chiral discrimination in terms of the ordering and geometry of the interconverting conformers. In a forthcoming publication we generalize the treatment of the chiral discrimination of flexible molecules, emphasizing the role of symmetry of both the individual conformers and of the interconversion process.

Acknowledgment. O.L. acknowledges French MNESER for a Ph.D. grant.

References and Notes

(1) Lesot, P.; Merlet, D.; Sarfati, M.; Courtieu, J.; Zimmermann, H.; Luz, Z. *J. Am. Chem. Soc.* **2002**, *124*, 10071.
(2) Collet, A. *Tetrahedron* **1987**, *43*, 5725.
(3) Salmon, M.; Cabrera, A.; Zavala, N.; Espinosa-Pérez, G.; Cardenas. J.; Gavino, R.; Cruz, R. *J. Chem. Crystallogr.* **1995**, *25*, 759.
(4) Luz, Z.; Poupko, R.; Wachtel, E. J.; Zheng, H.; Friedman, N.; Cao, X; Freedmanm, T. B.; Nafie, L. A.; Zimmermann, H. Private communication, 2006.
(5) Sarfati, M.; Lesot, P.; Merlet, D.; Courtieu, J. *Chem. Commun.* **2000**, 2069 and references cited therein.
(6) Canlet, C.; Merlet, D.; Lesot, P.; Meddour, A.; Loewenstein, A.; Courtieu, J. *Tetrahedron : Asymmetry* **2000**, *11*, 1911.
(7) Collet, A. In *Comprehensive Supramolecular Chemistry*; Atwood, J. L., Davies, J. E. D., MacNicol, D. D., Vögtle, J., Lehn, J.-M., Eds.; Pergamon Press: Oxford, U. K., 1996; Vol. 6, p 281.
(8) Zimmermann, H.; Tolstoy, P.; Limbach, H.-H, Poupko, R.; Luz, Z. *J. Phys. Chem. B* **2004**, *108*, 18772.
(9) Altmann, S. L. *Proc. R. Soc., Ser. A* **1967**, *298*, 184.
(10) Lesot, P.; Sarfati, M.; Courtieu, J. *Chem.—Eur. J.* **2003**, *9*, 1724.
(11) Merlet, D.; Ancian, B.; Courtieu, J.; Lesot, P. *J. Am. Chem. Soc.* **1999**, *121*, 5249.
(12) Lafon, O.; Lesot, P.; Merlet, D.; Courtieu, J. *J. Magn. Reson.* **2004**, *171*, 135.
(13) Note that the ^{13}C signal assignment reported in Figure 4 of ref 1 is incorrect.
(14) Note the change of sign relative to the definition used in ref. 1.
(15) Emsley, J. W.; Lindon J. C. *NMR Spectroscopy Using Liquid Crystal Solvents*; Pergamon Press: Oxford, U. K., 1975; Chapter 2.
(16) Meddour, A.; Berdagué, P.; Hedli, A.; Courtieu, J.; Lesot, P. *J. Am. Chem. Soc.* **1997**, *119*, 4502.
(17) Emsley, J. W.; Lindon J. C. *NMR Spectroscopy Using Liquid Crystal Solvents*; Pergamon Press: Oxford, U. K., 1975; Chapter 6.
(18) Herzfeld, J.; Berger, A. F. *J. Chem. Phys.* **1990**, *73*, 6021.
(19) Poupko, R.; Luz, Z.; Spielberg, N.; Zimmermann, H. *J. Am. Chem. Soc.* **1989**, *111*, 6094.
(20) Merlet, D.; Emsley, J. W.; Lesot, P.; Courtieu, J. *J. Chem. Phys.* **1999**, *111*, 6890.
(21) Eliel, A. L.; Wilen, A. H. *Stereochemistry of Organic Compounds*; Wiley & Sons: New York, 1994.
(22) Emsley, J. W.; Lindon J. C. *NMR Spectroscopy Using Liquid Crystal Solvents*; Pergamon Press: Oxford, U. K., 1975; Chapter 1.
(23) Burnell, E. E.; de Lange, C. A. *Mol. Phys.* **1972**, *24*, 673.
(24) Emsley, J. W.; Luckhurst, G. R. *Mol.. Phys.* **1980**, *41*, 19.
(25) Burnell, E. E.; de Lange, C. A. *Chem. Phys. Lett.* **1980**, *76*, 268.
(26) *Nuclear Magnetic Resonance of Liquid Crystals*; Emsley, J. W., Ed.; NATO ASI Series C, Mathematical and Physical Sciences 141; D. Reidel Publishing Company: Dordrecht, The Netherlands, 1983; Chapter 2.
(27) Emsley, J. W.; Lesot, P.; Merlet, D. *Phys. Chem. Chem. Phys*. **2004**, *6*, 522.